Measurement of air flow and blade loading at a large-scale cooling system fan

Jacques Muiyser[a], Danie N.J. Els[a], Sybrand J. van der Spuy[a] and Albert Zapke[b]

Received 4 December 2013, in revised form 2 June 2014 and accepted 13 June 2014

Axial flow fans installed at large-scale air-cooled condensers (ACCs) may operate under distorted inlet air flow conditions. These inflow conditions as well as the fan's surroundings cause a variation in blade loading as a function of the blade's rotational position. An investigation was launched to simultaneously measure the inlet air flow and the resultant blade and gearbox loading conditions of a single fan located on the edge of a large-scale ACC. Measurements were recorded over a period of five days where it was found that the air flow through the fan is highly dependent on the wind speed and direction. Subsequently, the pressure rise over the fan, which affects the blade loading, is highly dependent on the atmospheric wind speed and direction as well. In addition, the fan blade was found to vibrate at its own natural frequency of approximately 6 Hz when excited by the aerodynamic loading.

Additional keywords: axial flow fan, air-cooled condenser

Nomenclature

Roman

d	shaft diameter [m]
E	modulus of elasticity [N/m^2]
F	force [N]
G	torsional rigidity [N/m^2]
Q	shaft torque [N/m^2]

Greek

ε	linear strain [m/m]
γ	shear strain [m/m]
σ	bending stress [N/m^2]
Ω	fan rotational frequency [Hz]
τ	shear stress [N/m^2]
ω	frequency [Hz]

Subscripts

n	natural

1 Introduction

In coal-fired power stations water is boiled to produce steam that drives turbines which generate electricity. To complete the cycle the steam is condensed using either water or ambient air which is known as wet or dry cooling, respectively. This is known as the Rankine cycle. In arid regions where there is very little cooling water available an air-cooled steam condenser (ACC) is often used for the purpose of dry cooling[1].

Figure 1 shows a typical coal-fired power station with the dimensions similar to those of the ACC on which this investigation is focused. The layout of a typical fan unit located on the edge of such an ACC is shown in Figure 2. In this case the diameter of the fan is 9.145 m and it is situated at a platform height of 50 m. As shown in figure 2, the fan rotor is suspended from a fan bridge which also serves as a mounting platform for the electric motor and gearbox.

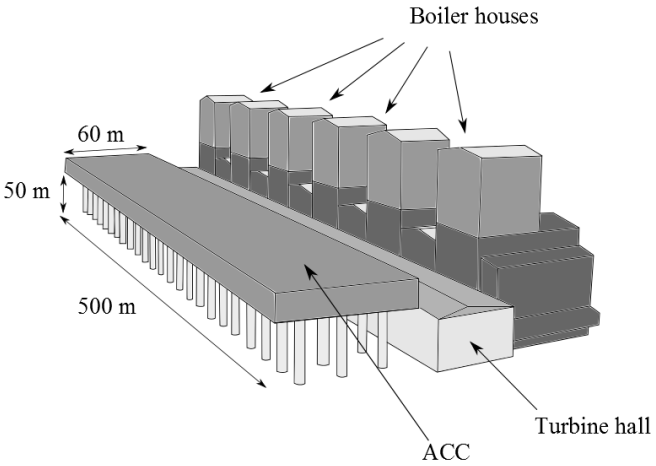

Figure 1 Typical coal-fired power station with ACC

Fan units located at the edge of an ACC often experience distorted inlet air flow conditions due to strong winds or other fans drawing air past them. Salta and Kröger[2] showed that by lowering the platform height, the air flow through edge fans is reduced due to the increase in cross-flow velocity. Thiart and Von Backström[3] placed an axial flow fan within the side wall of a wind tunnel, with its axis perpendicular to the tunnel's air flow direction, to investigate the effect of cross-flow on the fan's performance. Visser[4] later found that a large amount of cross-flow reduced the air flow through the fan. Stinnes and Von Backström[5] used angled inlet pipes to induce off-axis air flow into an axial flow fan and found that off-axis inlet air flow adversely affects fan pressure rise.

By using the numerical fan model developed by Meyer and Kröger[6], Hotchkiss *et al*.[7] confirmed the results obtained experimentally by Stinnes and Von Backström[5] and also found that off-axis inlet air flow causes a variation in fan blade thrust and torque at different azimuthal positions.

Bredell *et al.*[8] later conducted an investigation in which the variation in fan blade loading experienced by an ACC edge fan as a function of its rotational position when subjected to cross-flow conditions was determined numerically. These researchers modelled a section of an ACC containing two fans, one of which was an edge fan. The researchers then altered the amount of cross-flow at the edge fan's inlet by adjusting the platform height. By

a. Department of Mechanical and Mechatronic Engineering, University of Stellenbosch, Private Bag X 1, Matieland, 7602, South Africa, E-mail: 14903709@sun.ac.za
b. GEA Aircooled Systems (PTY) Ltd, P.O. Box 1427, Germiston, 1400, South Africa, E-mail: albert.zapke@gea.com

http://www.saimeche.org.za (open access) © SAIMechE All rights reserved.

reducing the platform height the cross-sectional area through which the inner fan draws in air is reduced and as such the cross-flow velocity at the edge fan inlet is increased. In this way it was found that the bending moments at the blade root increase as the blade approaches the windward side of the casing and that the increase in blade loading as a result of the distorted inlet air flow conditions can be up to 60% of the average blade load. This variation in aerodynamic loading then causes the fan blades to vibrate, which requires appropriate fatigue analysis of the components to determine if cyclical loading can lead to fatigue damage and possible component failure.

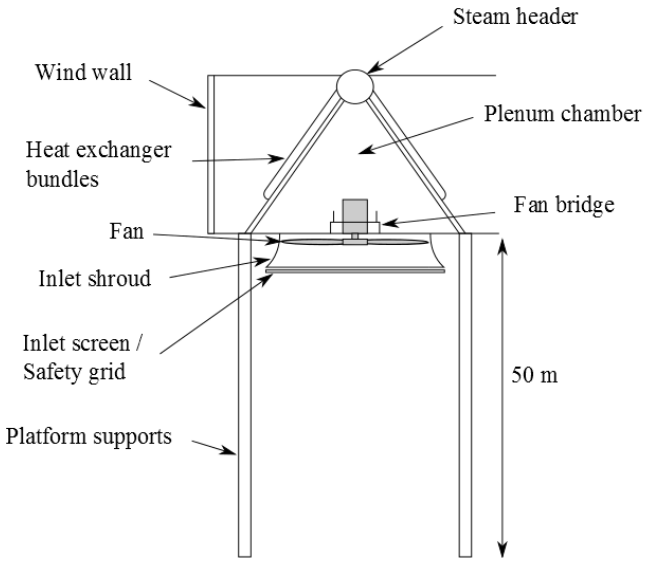

Figure 2 Typical ACC fan unit

Investigations that include measurements at full-scale ACCs are not as abundant as their numerical counterparts due to the high cost and increased difficulty of conducting such tests. Van Aarde[9] measured air flow and inlet temperature at the fans of a full-scale ACC by attaching propeller anemometers to a beam placed at the fan inlet. The beam was fixed at the centre and extended to the outer radius of the fan. A servo motor then stepped the beam through a number of azimuthal positions where measurements were recorded. These measurements provided an indication of the steady air flow at the fan inlet. Van Aarde[9] also measured the distribution of air pressure at the fan outlet but his work did not include any fan blade or gearbox loading measurements. The purpose of this investigation is therefore to include blade and gearbox loading measurements and to correlate these with real-time air flow measurements.

2 Experimental configuration

A system was developed to simultaneously record measurements of the fan blade and gearbox loading as well as the air flow conditions at the fan inlet. Once developed and tested, the measurement system was installed on the full-scale 9.145 m diameter axial flow fan that forms part of a 288-fan ACC.

2.1 ACC orientation and fan position

As shown in figure 3 the ACC is oriented with its windward side facing approximately east. A fan was selected near the longitudinal centre of the ACC because it was assumed that a fan located at the centre of the ACC would have primarily two-dimensional air flow at its inlet, as opposed to a fan located on a corner of the ACC where the air flow could be 3-dimensional[10].

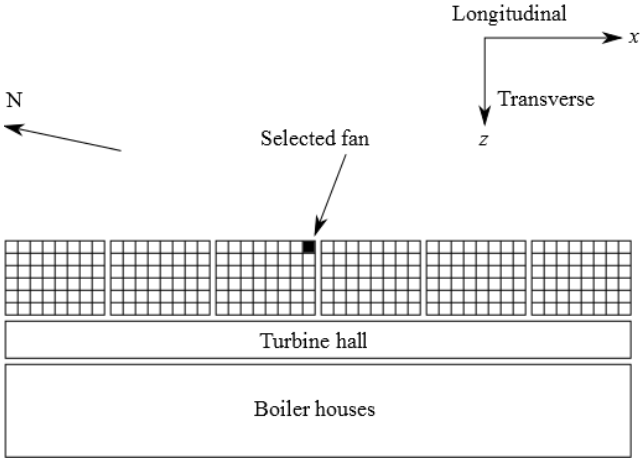

Figure 3 Location of instrumented fan within the ACC

2.2 Load measurements

Strain gauges were used to measure the loads at the fan blade neck as well as low-speed gearbox shaft. At the neck the strain gauges were attached to measure the bending strain in the flap- and lag-wise directions as well as the torsional strain. Similarly, strain gauges were attached to the gearbox shaft to measure bending strain in two directions, 90° apart. Figure 4 shows how the two sets of gauges were placed on the fan blade and gearbox shaft to measure the components of bending strain caused by the applied loads F1 and F2 while figure 5 and figure 6 show the strain gauges attached to the fan blade and shaft, respectively.

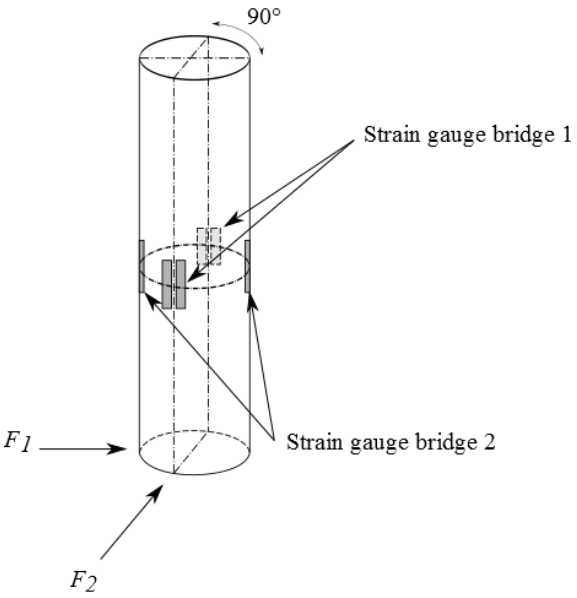

Figure 4 Strain gauge configuration for measuring bending at the blade neck and gearbox shaft

 © SAIMechE All rights reserved.

The strain gauges were calibrated using the functionality of the data capturing system discussed in section 2.5. However, at the blade neck the strain measurement itself was not of interest. Instead, it was important to equate the measured strain to an applied bending load. Without adjusting the blade angle, a ratchet strap was placed over the fan blade and fastened to the safety grid below. A load cell was placed on one end of the ratchet strap between the strap and the grid. The strap was tightened and the load cell used to determine the applied load. In this way a linear relationship between the applied bending moment and measured bending strain in the flap- and lag-wise directions was determined. The lag-wise direction is defined as being in the direction of the blade chord at its shoulder and the flap-wise direction perpendicular to this. For the gearbox shaft, loads could be calculated directly from the measured strain as the shaft's material and sectional properties were known.

Figure 5 Strain gauges attached to fan blade

Figure 6 Strain gauges attached to fan shaft

2.3 Inlet air flow measurements

A combination of ultrasonic and propeller anemometers were used to measure the inlet air flow conditions. Ultrasonic anemometers were chosen due to their fast response time. The GILL WindSonic two-axis anemometers that were used can record measurements at a rate of 5 Hz and as such are well suited to capture the effects of wind gusts.

A total of 6 measurement stations were constructed and fastened to the safety grid at the fan inlet. The measurement stations were equispaced along the centreline of the fan in the transverse direction of the ACC. Each measurement station, shown in figure 7, had a two-axis ultrasonic anemometer that measured the air flow in the fan's axial direction (*y*-direction) as well as the air flow in the transverse direction of the ACC (*z*-direction). These anemometers were supplemented with R.M. Young Model 27106T propeller anemometers that were used to measure the third component of air flow velocity in the longitudinal direction of the ACC (*x*-direction).The recorded inlet air flow measurements could later be compared to wind data captured using the weather mast located on-site. The weather mast was located approximately 700 m west of the ACC and had anemometers and wind vanes to measure wind speed and direction at a height of 40 m.

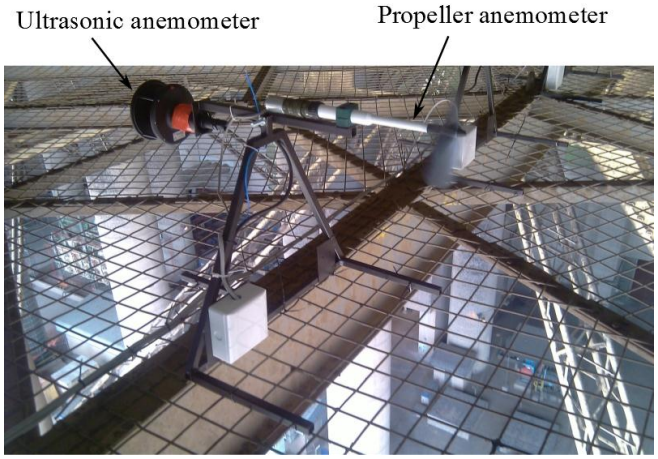

Figure 7 Inlet air flow measurement station

2.4 Fan blade position

To analyse the fan blade's response a position sensor was used to determine the fan blade's rotational position. The position sensor consisted of a Hall-effect proximity sensor located above the coupling flange between the fan shaft and hub. A metallic protrusion was attached to the top of one of the flange bolts in such a way that the proximity sensor would generate a signal each time the fan blade passes the 0° position, as denoted by figure 8. The position sensor configuration is shown in figure 9.

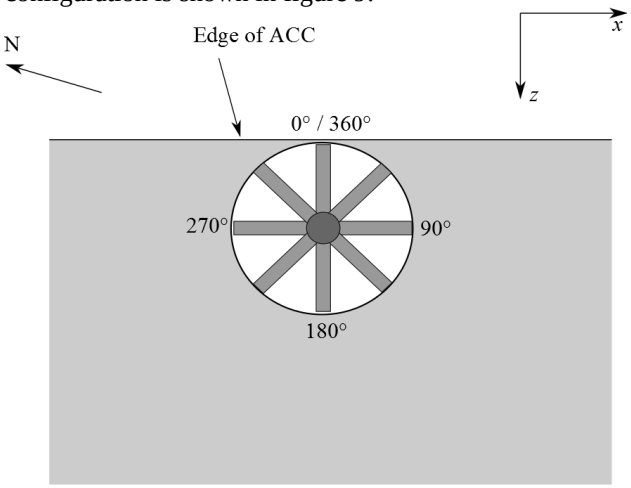

Figure 8 Directional convention and blade positions.

 © SAIMechE All rights reserved.

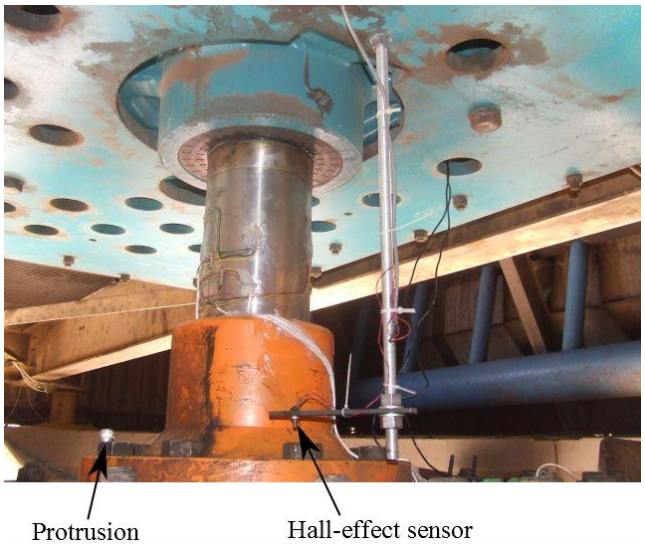

Figure 9 Fan blade position sensor

2.5 Data capturing system

An overview of the data capturing system is provided in figure 10. To capture strain gauge measurements from the rotating fan, MicroStrain V-Link wireless bridge amplifiers were used. Two units were used to capture the data from the six sets of strain gauges and were attached to the hub of the fan. These units each transmitted data to their own respective base stations which were connected to the rest of the data capturing system.

The analogue output signals created by the MicroStrain base stations as well as the analogue signals from the measurement stations were captured by two HBM QuantumX MX1601 units. These units were connected to an HBM QuantumX CX22W data recorder that synchronised and recorded all of the measurements.

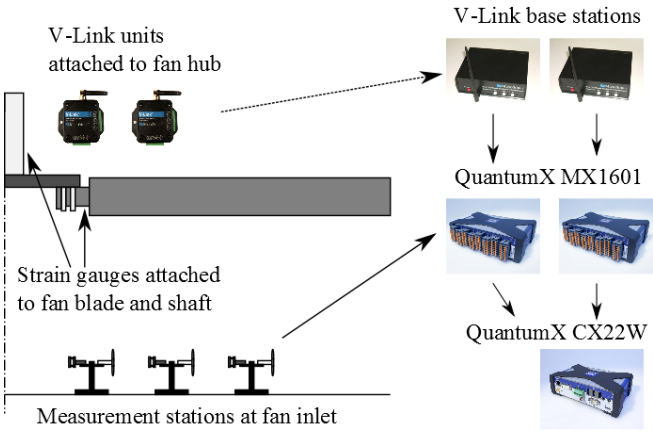

Figure 10 Overview of measurement system

3 Measurement results

3.1 Summary of recorded measurements

The measurements recorded over the 5 day period starting on 18/11/2011 are shown in figures 10 to 14 and summarised in table 1. In these figures the air flow and loading conditions are the average amounts calculated using a Hamming window with a 1 min length. Also, the location of each inlet air flow measurement station is referenced according to the distance along the *z*-axis with the peripheral side of the fan being at 0 m. Therefore, the 7.870 m location refers to the measurement station placed closest to the turbine hall, 7.870 m away from the peripheral side of the fan.

Table 1 Summary of daily measurements

	Day 1	**Day 2**	**Day 3**	**Day 4**	**Day 5**
Date	18/11/2011	19/11/2011	20/11/2011	21/11/2011	22/11/2011
Figure	11	12	13	14	15
Wind speed	5 m/s reducing to 2 m/s after 15:00	between 5 m/s and 10 m/s until 17:00 with a large increase of up to 20 m/s	average of 7 m/s decreasing to 5 m/s	between 5 m/s and 10 m/s reducing to between 0 m/s and 5 m/s	between 5 m/s and 10 m/s
Wind direction	N to NE with some scatter	primarily NW with a change to NE after 17:00	between N and NW with scatter turning to between N and SW	mostly NE with scatter to N and SE	mostly N
Air flow through fan (*y*-direction)	between 0 m/s and 5 m/s increasing to 5 m/s at 16:00	between 0 m/s and 5 m/s until 17:00 then between 5 m/s and 15 m/s	between 0 m/s and 5 m/s with a large deviation after 17:00	between 5 m/s and 10 m/s	between 2 m/s and 10 m/s
Average flap-wise blade loading	reduced from 5.5 kN.m to 4.7 kN.m	6.0 kN.m with a drop to 5 kN.m after 17:00	reduced from 6.5 kN.m to 5.5 kN.m	approximately 5.7 kN.m	6 kN.m reducing to 5.5 kN.m at 15:30 and increasing again to 6 kN.m

 © SAIMechE All rights reserved.

3.2 The effect of wind speed and direction on inlet air flow

Windy conditions causes cross-flow at the fan inlet and affects the air flow into the fan. On day 2 the wind blew from the north-west until approximately 17:00 where it suddenly shifted to an easterly direction and increased in speed. While the wind was blowing from the north-west the air flow into the fan was higher on the peripheral side than on the turbine hall side. After 17:00, in addition to an increase in air flow velocity on both sides of the fan, the air flow on the turbine side exceeded the air flow on the peripheral side.

A similar trend in air flow distribution can be seen in the data collected on day 3 and day 4. On day 3 the wind was blowing from the north-west until 13:00 when it shifted to a more westerly direction. The corresponding air flow through the fan after the shift was higher on the peripheral side of the fan than on the turbine hall side.

In contrast, the wind on day 4 was blowing from the north-east where it resulted in higher air flow on the turbine hall side than on the peripheral side of the fan. As such, the distribution of air flow into the fan in the *y*-direction is highly dependent on the prevailing wind direction with winds from the East causing higher flow into the turbine side of the fan and winds from the West resulting in the opposite.

In addition to the distribution of air flow into the fan, on days with easterly winds the average flow velocity into the fan was higher than on days when the wind was blowing from the west with the same velocity. This can be seen on day 4 where the average air flow through the fan was between 5 m/s and 10 m/s with an easterly wind of approximately 4 m/s while on day 3 the average air flow was only between 0 m/s and 5 m/s with a westerly wind of approximately the same magnitude. Similarly, on day 1 and day 2 changes in wind direction from a westerly to an easterly direction caused increases in air flow through the fan.

Increased wind speed also had the effect of causing increasing air flow into the fan on day 2 where the air flow into the fan increased with the large increase in wind speed.

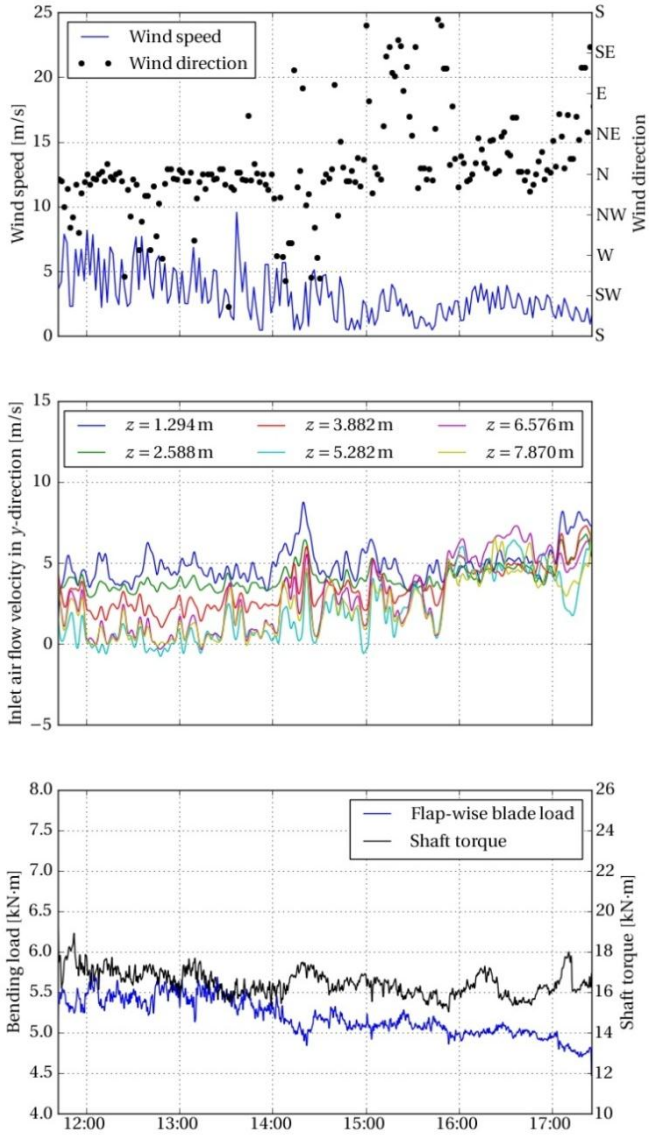

Figure 11 Measurements recorded on day 1

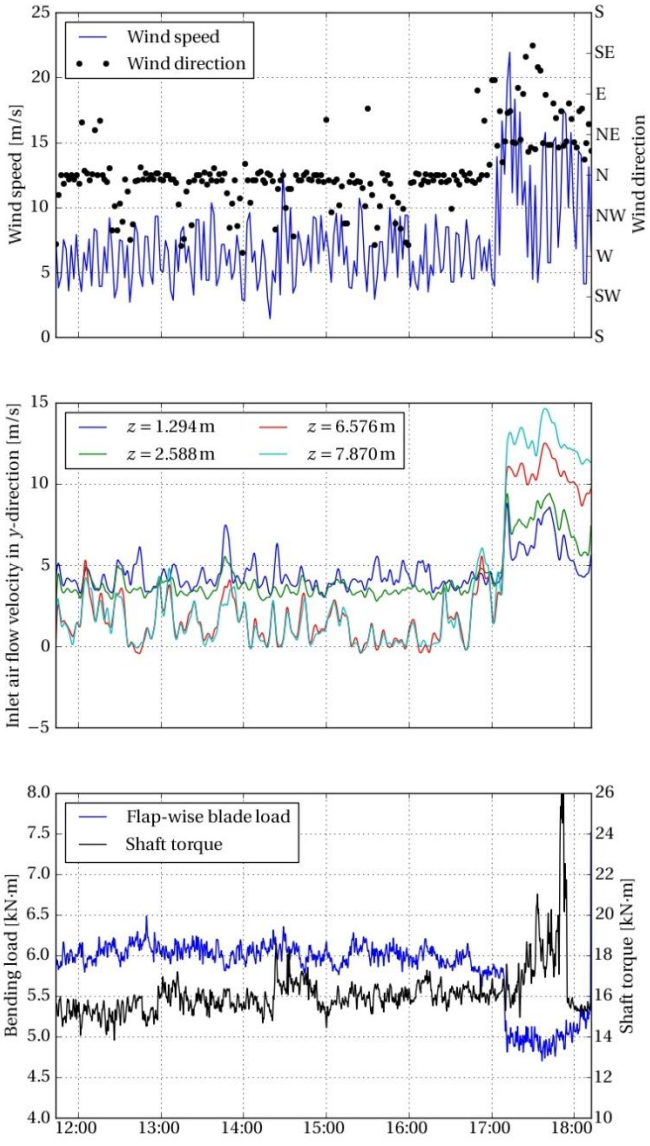

Figure 12 Measurements recorded on day 2

Additionally, the wind was blowing from approximately the same direction, but at a much higher speed on day 5 than on day 3 which resulted in the air flow through the fan being higher on day 5 than day 3.

3.3 Average blade loading

Fan blade loading is dependent on the relative angle at which the flow approaches and leaves the fan blade. These flow angles are influenced not only by the volume flow rate of air through the fan, but also the inflow conditions. Figure 16 shows that increased air flow results in a reduced static pressure rise over the fan[11]. Assuming that blade loading is proportional to fan static pressure rise, it can be deduced that increased air flow through the fan results in reduced blade loading.

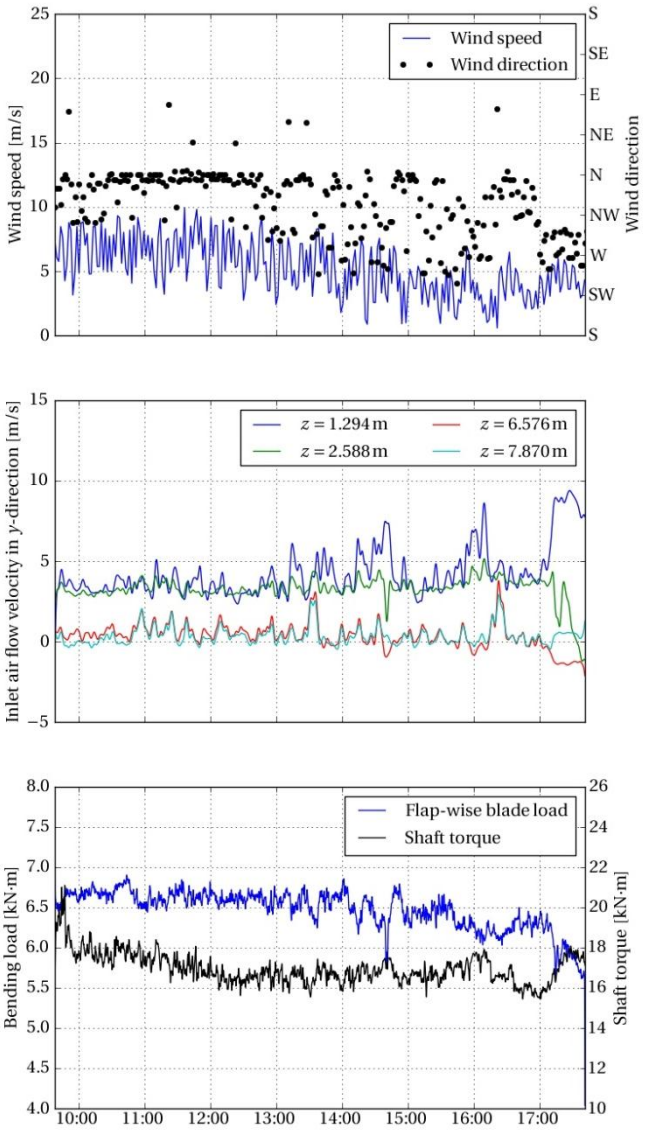

Figure 13 Measurements recorded on day 3

Measurements taken on day 2 best represent the effect that increased air flow has on blade loading. The average loading in the flap-wise direction was 6 kN.m until approximately 17:00, after which it dropped to 5 kN.m. This drop in loading corresponds with the sudden increase in air flow at the same time.

The air flow on day 1 exhibits a similar trend where during the course of the day the air flow through the fan gradually increased which caused a similarly gradual decrease in the average flap-wise blade loading.

Similar trends can also be found when comparing the measurements recoded on day 3, day 4 and day 5. The air flow into the fan was lower on day 3 than on day 4 and day 5, which resulted in a higher average bending load exerted on the fan blade.

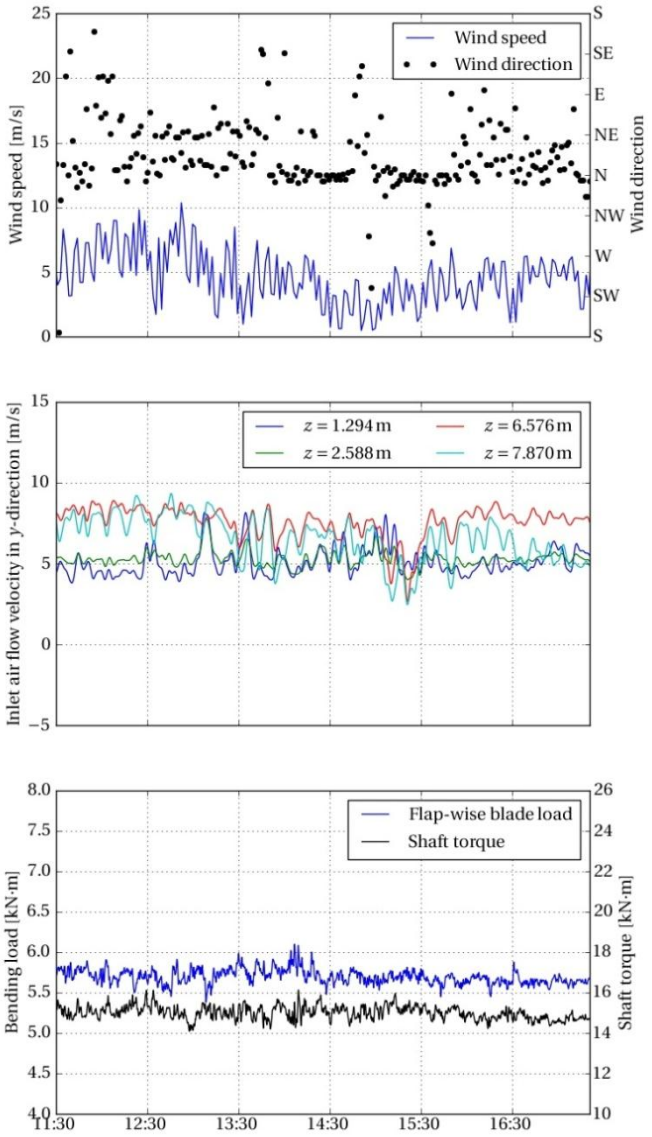

Figure 14 Measurements recorded on day 4

3.4 Blade loading amplitudes

As with the average blade loading, the loading amplitudes are also affected by the inlet air flow distribution. If the inlet air flow is not uniform, the aerodynamic forces exerted on the fan will vary depending on the blade's rotational position. This variation in blade loading then causes the fan blade to vibrate.

 © SAIMechE All rights reserved.

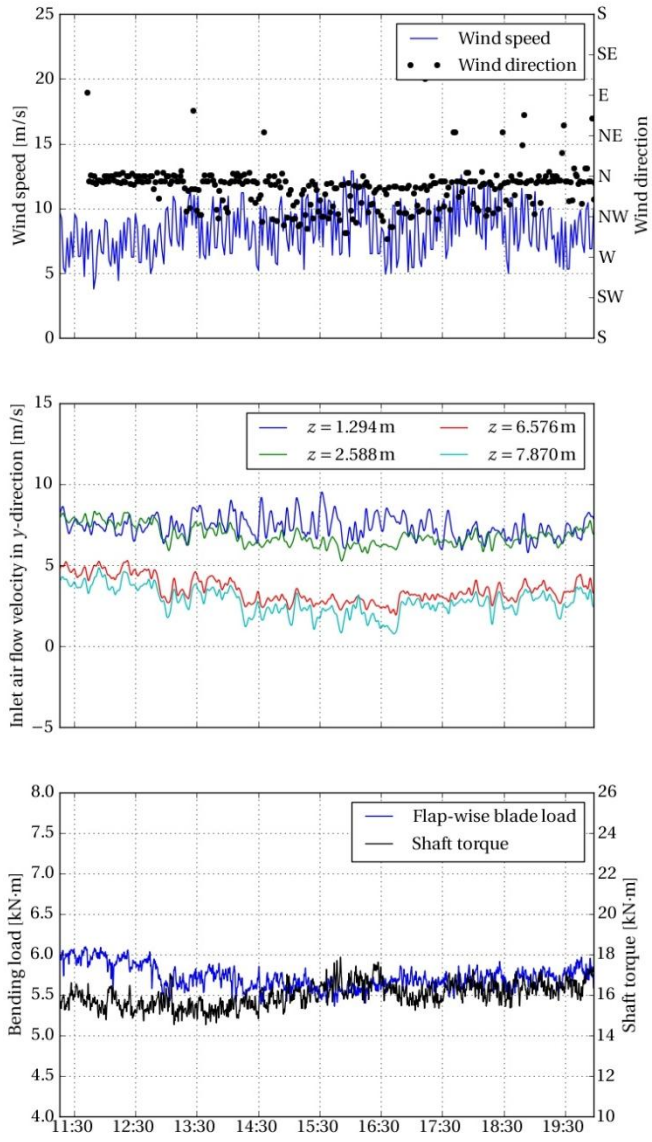

Figure 15 Measurements recorded on day 5

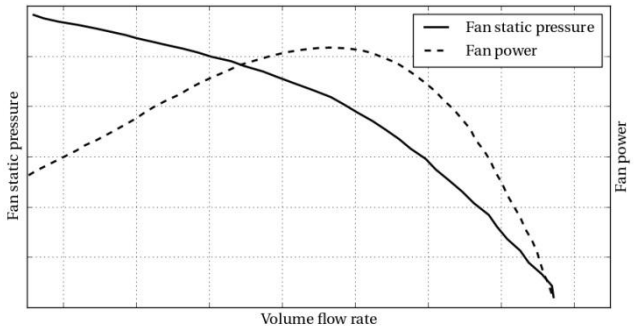

Figure 16 Typical fan performance curve[11]

Figure 17 shows the instantaneous bending data measured in the flap-wise direction on day 1. The blade loading had a maximum of approximately 12 kN.m and a minimum of -1 kN.m until 14:00 when these respective values decreased to 10 kN.m and 0 kN.m. Figure 18 shows the corresponding air flow measured in the *x*-direction on day 1 where the air flow recorded at most of the measurement stations dropped to 0 m/s at 14:00 and 17:00. At both of these times the blade loading amplitude decreased and as such the conclusion can be made that the blade loading amplitude is a function of the cross-flow at the fan inlet. This behaviour can be explained by considering that under cross-flow conditions, the fan blade will experience a variation in relative velocity depending on its rotational position. At some points the blade will be moving in the same direction as the air flow, resulting in a lower relative velocity than when the blade is moving in the opposite direction to the cross-flow. A large variation in blade loading will consequently result in larger loading amplitudes.

Furthermore, when operating under cross flow conditions, edge fans have been found to exhibit inlet side flow separation vortices[12]. These vortices would result in large load variations and is expected to increase the loading amplitude considerably. However, accurately measuring this phenomenon would require a large amount of sensors located at the peripheral side of the fan and was as such not within the scope of this project.

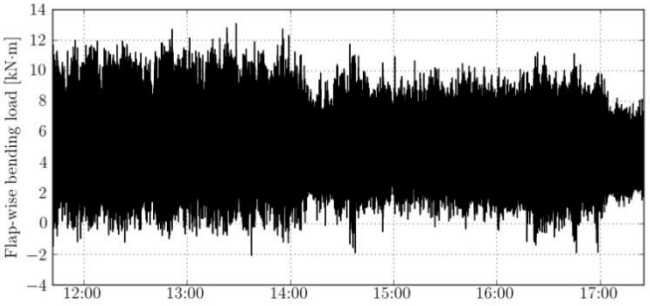

Figure 17 Flap-wise bending load measured on day 1

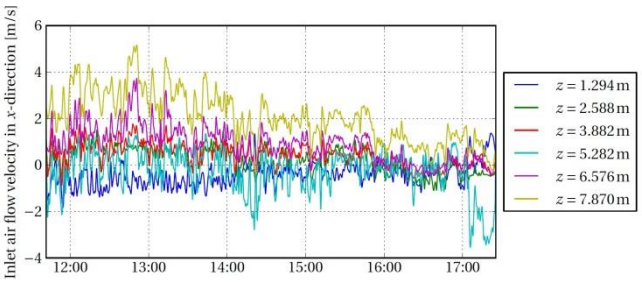

Figure 18 Inlet air flow measurements on day 1

3.5 Gearbox low-speed shaft torque

As a result of the variation in blade loading brought about by disturbed inlet air flow conditions, it is expected that the loads exerted on the fan gearbox will also vary. Gearbox loading is determined by analysing the bending and torque of the low speed fan shaft. Conversion from the measured torsional strain to shaft torque can be accomplished using equation 1 with the torsional rigidity of steel taken as 79.3 GPa[13].

$$Q = \frac{\pi \gamma G d^3}{16} \quad (1)$$

Figure 11 shows the shaft torque on day 1. The approximate torque for the duration of the day was 16 kN/m with increases after 14:00 and 17:00. One can see that the increased torque occurred at the same time as the air flow

into the fan increased. Shaft torque measured on day 2 shows an increase after 17:00 that also coincides with an increase in air flow. These increases in shaft torque can be explained using of Figure 16 where, when below a certain value, any increase in air flow through the fan would result in an increase in fan power and consequently the torque exerted on the shaft.

3.6 Gearbox shaft bending stress

Bending stress is related to strain by equation 2. For all of the calculations performed, a modulus of elasticity of 207 GPa was used[13].

$$\sigma = \varepsilon \times E \quad (2)$$

Figure 19 shows the bending stress experienced by the fan shaft in one of the two measured directions on day 2. Only one of the two sets of data was plotted because when the data is viewed over a long time period the recorded measurements of the two separate channels appear to be exactly the same. The first observation regarding the measured stress is that there is a positive offset of approximately 30 MPa, which means that there is an imbalance in the fan rotor exerting a constant bending load on the shaft. The second observation is that the loading is not steady, but oscillates about the offset. The amplitude of oscillation also undergoes a sudden increase at 17:00, which coincides with the increase in air flow measured on the day. The increase in bending stress can be attributed to the fact that during the period of high air flow there was also a larger difference in air flow between the windward and turbine sides of the fan creating a large imbalance in fan blade loading.

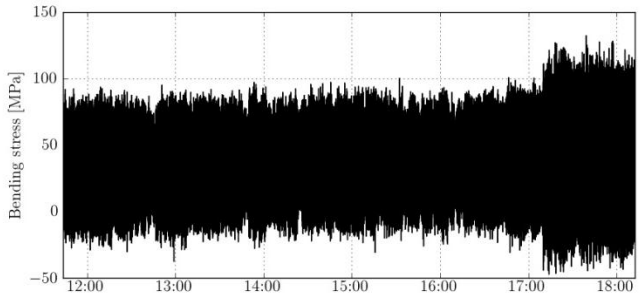

Figure 19 Shaft bending stress recorded on day 2

3.7 Dynamic analysis of blade loading

The data presented in figure 20 shows the resultant blade bending loads measured for a period of 2 s on the fan rotating at 125 rpm. Each solid vertical line represents a point in time that a pulse was generated by the position sensor due to the fan blade passing the 0° position. From the recorded data it can be seen that the blade loading is cyclical.

During each revolution, the fan blade experiences a peak bending load at the 0° position with two other peaks appearing at approximately 90° and 225°. The fan rotates in a clockwise direction and as such it is expected that the loading between 0° and 180° would be lower than the loading between 180° and 360° because the cross-flow at the fan inlet is generally in the positive *z*-direction. While the blade is between 0° and 180°, it is moving in the same direction as the air flow and when the blade is between 180° and 360° it is moving against the air flow. When the blade is moving against the air flow, there is a higher angle of attack over the blade which causes higher blade loading. This effect is shown in the measured data where it can be seen that the average blade loading increases as the blade completes a revolution.

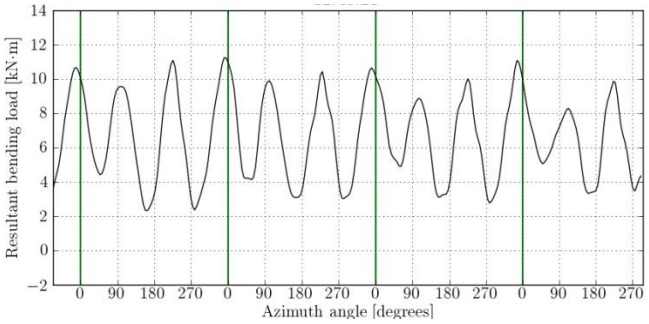

Figure 20 Shaft bending stress recorded on day 2

Figure 21 shows a fast Fourier transform (FFT) of the blade loading data recorded on day 2 where the dominant frequencies are 2 Hz, 4 Hz and 6 Hz. The 2 Hz frequency is approximately equal to the rotational frequency of the fan while the frequency at 4 Hz is the frequency at which the blade passes beneath the fan bridge. The frequency at 2 Hz can be attributed to the aforementioned once-per-revolution load variation exerted on the fan blade as it rotates. The frequency at 6 Hz can be attributed to the blade's first natural frequency of approximately 5.9 Hz[14]. When considering the measured data, it can be seen that the dominant vibration is as a result of the blade oscillating at its own natural frequency.

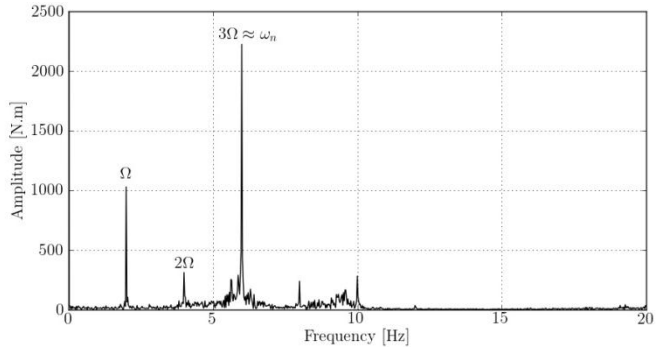

Figure 21 Shaft bending stress recorded on day 2

4 Conclsion

The objective of the study was to develop a system that could simultaneously measure the inlet air flow and mechanical loading on the fan rotor and gearbox of a large-scale ACC fan unit. Measurements were then recorded from an array of sensors and weather mast located on-site over a period of five days in November 2011.

Analysis of the recorded measured data yielded the following conclusions:

1. Winds blowing from the west caused higher air flow through the peripheral side of the fan while winds blowing from the east resulted in higher air flow on the turbine side of the fan.

2. Air flow through the fan was higher on days where the wind was blowing from the east than on days that the wind was blowing from the west.
3. Average blade loading was calculated for each of the 5 measurement days where it was found to vary between 5 kN.m and 6.5 kN.m, depending on the inlet air flow conditions. Higher air flow velocities in the axial direction of the fan resulted in lower flap-wise bending loads.
4. The fan blade was found to vibrate at its own natural frequency of approximately 6 Hz while a second dominant loading frequency was found at the rotational frequency of the fan, which is a result of the blade experiencing changes in aerodynamic loading as it rotates. It should be noted that the loading profiles that were obtained are only valid for the case in which the fan blade's first natural frequency is approximately three times the rotational speed.
5. The minima and maxima of the measured blade loading remained between -2 kN.m and 14 kN.m, respectively, for all of the measurement days. However, a reduction in cross-flow at the fan inlet caused this range to decrease.

Finally, the primary objective of this investigation was the development of a measurement system capable of simultaneously measuring air flow and loading conditions of the gearbox and fan blades. The relationships between these measurements are based on data that was recorded over a short time period and as such cannot be used to draw definitive conclusions regarding the behaviour of the system. It fell outside the scope for this particular project, but due to the inherent uncontrollability of environmental effects as well as the sheer volume of interacting factors, it is recommended that similar research be conducted over a much longer period of time at more than one fan.

5 Acknowledgements

The financial assistance of the National Research Foundation (NRF) towards this research is hereby acknowledged. Opinions expressed and conclusions arrived at, are those of the author and are not necessarily to be attributed to the NRF.

GEA Aircooled Systems and Howden Fan Equipment are thanked for their financial and technical contributions.

References

1. *Kröger DG,* Air-cooled Heat Exchangers and Cooling Towers, PennWell Corporation, Tulsa, 2004.
2. *Salta CA and Kröger DG,* Effect of inlet flow distortions on fan performance in forced draft air-cooled heat exchangers, *Heat Recovery Systems and CHP*, 1995, 15, 555-561.
3. *Thiart GD, and von Backström TW,* Numerical Simulation of the flow field near an axial fan operating under distorted inflow conditions, *Journal of Wind Engineering and Industrial Aerodynamics*, 1993, 45, 189-214.
4. *Visser J,* Die invloed van versteurde inlaatvloeipatrone op aksiaalwaaiers, MScEng thesis, Department of Mechanical and Mechatronic Engineering, University of Stellenbosch, South Africa, 1990.
5. *Stinnes WH and von Backström TW,* Effect of cross-flow on the performance of air-cooled heat exchanger fans, *Applied Thermal Engineering*, 2002, 22, 1403-1415.
6. *Meyer CJ and Kröger DG,* Numerical simulation of the flow field in the vicinity of an axial flow fan, *International Journal for Numerical Methods in Fluids*, 2001, 36, 947-969.
7. *Hotchkiss PJ, Meyer CJ and von Backström TW,* Numerical Investigation into the effect of cross-flow on the performance of axial flow fans in forced draught air-cooled heat exchangers, *Applied Thermal Engineering*, 2006, 26, 200-208.
8. *Bredell J, Kröger DG and Thiart G,* Numerical investigation into aerodynamic blade loading in large axial flow fans operating under distorted inflow conditions, *R&D Journal of the South African Institution of Mechanical Engineering*, 2006, 22, 11-17.
9. *Van Aarde D,* Vloeiverliese deur 'n A-raam vinbuisbundel in 'n lugverkoelde kondensator, MScEng thesis, Department of Mechanical and Mechatronic Engineering, University of Stellenbosch, South Africa, 1990.
10. *Van Rooyen J,* Performance trends of an air-cooled steam condenser under windy conditions, MScEng thesis, Department of Mechanical and Mechatronic Engineering, University of Stellenbosch, South Africa, 2007.
11. *Kröger DG,* Fan performance in air-cooled steam condensors, *Heat Recovery Systems and CHP*, 1994, 14, 391-399.
12. *Van der Spuy SJ, Von Backström TW and Kröger DG,* An evaluation of simplified methods to model the performance of axial flow fan arrays, *R&D Journal of the South African Institution of Mechanical Engineering*, 2009, 26, 12-20.
13. *Budynas RG and Nisbett JK,* Shigley's Mechanical Engineering Design, 8th Edition, McGraw Hill, New York, 2008.
14. *Swiegers J,*Structural optimisation of a composite material fan blade using the finite element method, MScEng thesis, Department of Mechanical and Mechatronic Engineering, University of Stellenbosch, South Africa, 2012.